

Politecnico di Torino

Politecnico di Torino

Master's Degree in Industrial Environmental Sustainability
Environmental and Territorial Engineering
A. y. 2025/2026
Graduation Session September 2026

Experimental characterization of hydrated lime sorbents for acid gas adsorption

Supervisors:

Marco Ravina
Mariachiara Zanetti
Deborah Panepinto

Candidate:

Edoardo Gennaro

Dedicata al Nostro pianeta Terra.
Dopo tutto ciò che mi hai dato nel corso della vita, è finalmente giunto il momento che provi a ricambiare il favore.

ABSTRACT

Hydrochloric acid (HCl) represents one of the main acidic pollutants present in flue gas produced by waste incineration plants and by many industrial processes. Its removal has a fundamental role for both the compliance with emission limits and the corrosion and degradation phenomena within industrial plants. Among the used reagents used in dry systems for the abatement of HCl, hydrated lime is one of the most diffused solutions thanks to its low cost and to its good reactivity towards acid gases.

The present thesis work aimed to compare the behaviour of two different samples of hydrated lime, named C1 and C3, characterised by different magnesium contents and physical properties, with the aim of evaluating their HCl adsorption capability and correlating their performances with the physicochemical characteristics of the materials.

The experimental activity was conducted using a laboratory plant in which the gaseous mixture containing HCl was passed through a lime bed maintained at a controlled temperature. The adsorption capacity was evaluated through dissolution tests on the reacted samples followed by ion chromatography analyses, while the characterisation before and after the reaction was carried out through BET, ICP-OES and XRD analyses.

The results highlighted a rapid adsorption in the initial phases of the tests, followed by a progressive reduction of the reaction rate,

attributable to the formation of reaction products and to the consequent reduction of the available porosity. The BET analyses confirmed a marked reduction of the specific surface area and of pore volume in the reacted samples, while the ICP analyses highlighted modifications at chemical level associated to the adsorption process. From the comparison on the two materials, it emerged how the C3 sample presented, in the majority of the investigated experimental conditions, a slightly higher adsorption capability than the C1 sample, suggesting a possible positive contribution from the higher magnesium content, despite its lower initial specific surface area.

Overall, the work enabled a deeper understanding in the interaction mechanisms between HCl and hydrated lime, highlighting the role of the physicochemical characteristics of the sorbent on the abatement performances and giving useful indications for future developments and optimisation of the materials used in gas purification systems.

TABLE OF CONTENTS

CHAPTER 1: INTRODUCTION 1

1.1 The Problem of acid gas pollution 1

1.1.1 Acid gas origin 1

1.1.2 Environmental impact 2

1.1.3 Industrial and plant impact 2

1.2 Hydrochloric acid pollution 3

1.2.1 Origin and generation mechanisms 3

1.2.2 Health and environmental impact: acid rain 3

1.2.3 Industrial impact: corrosion and fouling 4

1.2.4 Speciation of other pollutants 4

1.2.5 Distribution of chlorine at the plant outlet 5

1.3 Technologies for the abatement of hydrochloric acid 5

1.3.1 Wet Scrubbing 5

1.3.2 Semi-wet Scrubbing 6

1.3.3 Dry Sorbent Injection (DSI) 7

1.3.4 Finishing technologies and combined systems 7

1.4 State of the art on the use of hydrated lime 8

1.4.1 Calcium-based reagents typologies 8

1.4.2 Application in different purification processes 8

1.4.3 Operative parameters and optimisation 9

1.4.4 Recirculation of residues 9

1.4.5 Comparison with sodium bicarbonate 10

1.5 Thesis objectives 10

CHAPTER 2: INSTRUMENTATION AND METHODS 11

2.1 Lime samples used 11

2.1.1 Chemical characteristics of the virgin samples 11

2.1.2 Mineralogical composition of the virgin samples 13
2.1.3 Surface area and pore volume of the virgin samples 15
2.2 Experimental plant 17
2.3 Experimental procedure 21
2.4 Methods for samples analysis 23
2.4.1 Blank tests 23
2.4.2 Absorption tests on the outlet mass 24
2.4.3 Dissolutions on the adsorbed mass 24
2.4.4 Physicochemical characterization of the reacted samples 25
CHAPTER 3: RESULTS AND DISCUSSION 26
3.1 Blank tests 26
3.2 Absorption tests on the outlet mass 27
3.3 Dissolution tests on the adsorbed mass 29
3.4 BET analysis 35
3.5 ICP analysis 36
3.6 Comparison between C1 and C3 samples 38
CHAPTER 4: CONCLUSIONS 40
REFERENCES BIBLIOGRAPHY 44

CHAPTER 1: INTRODUCTION

1.1 The Problem of acid gas pollution

Acid gases are a critical category of pollutant substances emitted from industrial combustion processes, especially waste incineration. This class of substances includes mainly sulfur dioxide (SO_2), hydrochloric acid (HCl) and hydrofluoric acid (HF). Hydrobromic acid (HBr) and hydroiodic acid (HI) are also considered acid gas pollutants (Neuwahl et al., 2010).

1.1.1 Acid gas origin

The formation of these gases is directly linked to the chemical composition of the combusted material and the operating conditions of the furnace (Neuwahl et al., 2010):

- **Hydrochloric acid:** it is generated by the combustion of wastes containing inorganic chlorides or chlorinated organic compounds. In urban sold waste (MSW), it has been estimated that about half of the chloride comes from PVC combustion. During the incineration, chloride is converted in HCl, which can later react with other inorganic compounds to generate volatile metallic chlorides.

- **Sulfur dioxide:** it comes from the sulfur present in the fuel or in the waste (such as paper, plasterboard or sewage sludge). Under specific reaction conditions, a part (about 5% at the inlet of purification systems) can be converted into sulfur trioxide (SO_3), a particularly critical compound for the formation of acidic condensates.

- **Hydrofluoric acid:** the generation mechanism is the same as for HCl, mainly coming from plastics, fluorinated fabrics or the decomposition of calcium fluoride (CaF_2).

While in coal-fired power plants the priority is the desulfurization (SO_2 removal), in waste incineration plants the attention is split between SO_2 and HCl, given the high concentration of the latter in raw flue gas (M. Giugliano; S. Cernuschi, 2014).

1.1.2 Environmental impact

Acid gas emissions into the atmosphere have harmful effects on different scales (Neuwahl et al., 2010):

- **Acidification and eutrophication:** SO_2 and other acid gases are precursors of acid rain. Once they are deposited, they change the pH of soil and water bodies, contributing to acidification phenomena that damage aquatic and terrestrial ecosystems.

- **Vegetation damage:** HF and HCl are highly soluble gases in water and they have a direct and negative impact on plant growth.

- **Secondary aerosols:** SO_2 is an essential precursor for the generation of secondary aerosols, which influence air quality and human health.

1.1.3 Industrial and plant impact

Other than environmental effects, the presence of acid gases brings serious problems to plant operation itself (Neuwahl et al., 2010):

- **High-temperature corrosion:** HCl is one of the main causes of the corrosion of metallic surfaces inside boilers and economizers, especially in the presence of ash deposits.

- **Acid dew point:** the presence of SO_3 and water vapor significantly increases the acid dew point of the flue gas. If the temperature of the flue gas goes below this limit, highly corrosive acidic condensates are generated, which can chemically attack filter fabrics and the metallic structures of the purification system. To

avoid such phenomena, the gas temperature must be kept at least 10-15°C above the dew point (M. Giugliano; S. Cernuschi, 2014).

1.2 Hydrochloric acid pollution

Hydrochloric acid (HCl) is considered the main pollutant in flue gas, with concentrations overcoming those of sulfure dioxide in plants treating municipal solid waste (M. Giugliano; S. Cernuschi, 2014). Its management is essential not only for the regulatory compliance, but also for maintaining the structural integrity of the entire system.

1.2.1 Origin and generation mechanisms

Hydrochloric acid is generated during the combustion phase because of the presence of chlorinated organic compounds or inorganic chlorides in the waste matrix. In the municipal solid waste (MSW) context, technical literature identifies a specific primary source: it has been estimated that about 50% of the chloride present in the waste comes from PVC (polyvinyl chloride) (Neuwahl et al., 2010).

During the thermal process, the organic component of these polymers is destroyed, releasing chloride atoms, which are converted into the gaseous phase. A part of this gas can later react with other inorganic components present in the burning bed to generate metallic chlorides, some of which are volatile and can be found in flue gas and in fly ash (Neuwahl et al., 2010).

The concentration of HCl in raw flue gas (before purification treatments) shows considerable variability based on the type of waste feed. For MSW incineration plants, the typical concentration is between 500 and 2,000 mg/Nm^3, while in hazardous waste plants the peaks can reach 100,000 mg/Nm^3, especially in the presence of waste stored in drums that release sudden waves of pollutants (Neuwahl et al., 2010).

1.2.2 Health and environmental impact: acid rain

Hydrochloric acid is a highly soluble gas in water. Given this physical property, once emitted into the atmosphere, HCl rapidly interacts with humidity, being removed by

wet deposition (acid rain) which can alter the pH of soil and water bodies (Neuwahl et al., 2010).

From an ecological point of view, HCl therefore has a direct and negative impact on plant growth. Furthermore, acidic emissions contribute to eutrophication phenomena and to the generation of secondary aerosols, which influence air quality at a regional level.

1.2.3 Industrial impact: corrosion and fouling

Even if HCl is an environmental pollutant, its most immediate and destructive effects are observed inside the plant itself. It is one of the main agents responsible for high-temperature corrosion, a phenomenon that attacks boiler pipes and economizers.

- **Chloride corrosion:** this mechanism is especially activated when chlorides are released during the sulfation of alkaline deposits on metallic surfaces, directly attacking iron or lead hydroxides. In incineration plants, this kind of corrosion has been commonly observed when flue gas temperatures are over 700°C (Neuwahl et al., 2010).

- **Acid dew point:** HCl contributes to increasing the temperature at which flue gas condenses into liquid acids. If the gas temperature falls below the acid dew point, hydrochloric acid droplets are generated. These droplets can chemically attack metallic materials and can clog filter fabrics of the purification system. Because of that, it is essential to keep the final temperature of the flue gas at least 10-15°C above the dew point (M. Giugliano; S. Cernuschi, 2014).

- **Fouling:** above 600-800°C, ashes containing chlorides can become sticky, promoting the accumulation of solid deposits (fouling) on heat-transfer surfaces, reducing the energy recovery efficiency (Neuwahl et al., 2010).

1.2.4 Speciation of other pollutants

Another important technical aspect is the interaction between hydrochloric acid and mercury. The presence of sufficient concentration of HCl in flue gas promote the conversion of elemental mercury (hard to break down) in mercuric chloride ($HgCl_2$),

an ionic form much more soluble and therefore easy to capture in wet washing systems or through adsorption on activated carbon (Neuwahl et al., 2010).

1.2.5 Distribution of chlorine at the plant outlet

Analysing the mass balance of a modern waste-to-energy plant, it can be noticed that the chlorine is removed from the flue gas with efficiencies of over 99% (Neuwahl et al., 2010). However, this means that the removed chlorine is concentrated into solid residues:

- about 35% of the total chlorine mass ends up in the electrostatic precipitator (ESP) dust;
- over 50% is transferred in wastewater (in wet systems) or to the solid residues from the purification process;
- less than 1% is finally emitted from the chimney as residual emissions, thanks to the high efficiency of the abatement technologies.

1.3 Technologies for the abatement of hydrochloric acid

The abatement of hydrochloric acid is mainly based on absorption operations, which consist of transferring the pollutant from a gaseous phase to a liquid (wet absorption) or solid (dry absorption) phase. Since HCl is a highly soluble and reactive gas, the technology selection depends on different factors such as the required efficiency, the variability of the inlet load, the cost of the reagents and the management of the produced residuals (M. Giugliano; S. Cernuschi, 2014).

1.3.1 Wet Scrubbing

Wet systems represent the technology that offers the highest removal efficiencies for soluble acid gases such as HCl. The process is based on the contact between the gas stream and a liquid sorbent (usually water or alkaline solutions) inside packed towers, plate columns or spray chambers (M. Giugliano; S. Cernuschi, 2014).

Mass transfer is described by the two-film theory, where the resistance is located at the gas-liquid interfaces. In the case of HCl, water solubility is so high that the

process is almost exclusively limited to the resistance in the gaseous phase, making the absorption extremely fast.

Typically, HCl is removed in the first washing stage, operating at a strongly acidic pH (pH 0-1). This condition allows the selectively removal of HCl (and HF) saturating the solution, while sulfur dioxide (SO_2) requires an extra stage operating at neutral or slightly alkaline pH (pH 6-7) to be effectively absorbed (Neuwahl et al., 2010).

The main advantage of this type of process is the low reagent consumption thanks to stoichiometric ratios close to unity (1.0-1.2). However, these systems produce liquid waste loaded with salts (chlorides) and heavy metals, which require complex physicochemical treatments before discharge or recirculation (Neuwahl et al., 2010).

1.3.2 Semi-wet Scrubbing

In these systems, the alkaline reactant is injected as aqueous suspension (typically lime slurry) or solution in the hot flue gases stream inside a spray reactor.

The water contained in the suspension completely evaporates thanks to the sensible heat of the flue gas, adiabatically cooling it down. The chemical reaction initially happens in the liquid phase of the nebulized droplets and continues on the surface of dry products generated during evaporation (M. Giugliano; S. Cernuschi, 2014).

The products of the reaction and the excess reagent are collected in a downstream baghouse filter, which works as a secondary reactor where the gas-solid contact continues through the dust layer accumulated on the filtering fabrics.

Compared to dry systems, the higher humidity and the initial liquid phase significantly improve the system's reactivity, allowing the use of a lower excess of reagent.

1.3.3 Dry Sorbent Injection (DSI)

Dry processes involve the direct injection of solid pulverized reagents, such as hydrated lime ($Ca(OH)_2$) or sodium bicarbonate ($NaHCO_3$), directly into the flue gas duct or in a dedicated reactor (M. Giugliano; S. Cernuschi, 2014).

Hydrated lime is the most common reagent because of its low cost. It often requires the use of high-specific-surface limes (HSS) to effectively operate at temperatures between 140°C and 150°C.

Sodium bicarbonate, on the other hand, offers a higher reactivity towards HCl, especially at temperatures between 160°C and 180°C. During the injection, sodium bicarbonate undergoes thermal decomposition which increases its porosity and specific surface (*popcorn* effect), accelerating the neutralization.

In these processes too, the efficiency is enhanced by the accumulation of the reagent on the baghouse filter. To reduce the fresh lime consumption, which often operates with high stoichiometric ratios (1.5-2.5), modern systems provide for the recirculation of solid residues, which are reactivated (sometimes with steam or humidification) and reinjected into the gas stream.

1.3.4 Finishing technologies and combined systems

In some plants, a double stage configuration or the addition of a polishing scrubber downstream of a dry system is adopted. The latter solution is used to guarantee compliance with emission limits even in the presence of high pollutant peaks in the combusted waste, combining the simplicity of a dry system with the reliability of wet scrubbers (Neuwahl et al., 2010).

Continuous upstream monitoring of HCl is a fundamental technique to optimise reagent dosing, allowing a quick response to load variations and, at the same time, reducing the production of non-reacted solid residues (Neuwahl et al., 2010).

1.4 State of the art on the use of hydrated lime

Among the available alkaline reagents, hydrated lime ($Ca(OH)_2$) represents one of the most widely used materials for the abatement of acid gases thanks to its low cost, its high availability and good reactivity towards HCl, HF and SO_2.

The removal mechanism is based on gas diffusion towards the particle surface and subsequent neutralization reaction. For hydrochloric acid, the main reaction can be described as:

$$Ca(OH)_2 + 2HCl \rightarrow CaCl_2 + 2H_2O$$

The overall efficiency of the process depends on many factors, such as temperature, relative humidity, contact time between the flue gas and the particle, pollutant concentration and the adsorbent's physical characteristics (M. Giugliano; S. Cernuschi, 2014).

1.4.1 Calcium-based reagents typologies

Based on the plant configuration, lime can be used in different forms (Neuwahl et al., 2010):

- **Standard hydrated lime:** mainly used in dry and semi-dry systems;
- **High-specific surface lime (HSS):** represents the most advanced technology on the market for dry systems. Thanks to a specific surface area and porosity much higher than those of standard lime, it guarantees high removal efficiencies even at higher operating temperatures (up to 160-180°C) and with shorter contact times;
- **Lime slurry:** an aqueous suspension of calcium hydroxide produced *in situ* through the hydration of quicklime (CaO), used in semi-dry systems (SDA - Spray Dryer Absorber) and in some stages of wet scrubbing.

1.4.2 Application in different purification processes

The state of the art includes the integration of lime in three main process configurations (Neuwahl et al., 2010):

- **Dry Sorbent Injection (DSI):** hydrated lime in powder form is directly injected in the flue gas duct. The neutralization reaction happens in solid phase and is completed on the baghouse filter surface, where the accumulated reagent's layer (cake) acts as a secondary reactor, increasing the contact time between gas and solid;
- **Semi-wet/semi-dry systems:** lime slurry is nebulized in a reaction chamber. Water evaporates, cooling down the flue gas, while the chemical reaction begins in the liquid phase of the droplets and continues on the dry salts which generated during evaporation. This technique offers better use of the reagent compared to the purely dry systems thanks to the higher humidity and initial reactivity;
- **Wet Scrubbing:** in multistage configurations, lime (or limestone) can be used in the second stage for SO_2 removal, operating at neutral pH (6-8) and leading to the formation of gypsum ($CaSO_4$), recoverable as an industrial by-product.

1.4.3 Operative parameters and optimisation

Hydrated lime efficiency is strictly connected to the monitoring of three fundamental parameters: temperature, humidity and stoichiometric ratio (M. Giugliano; S. Cernuschi, 2014).

In dry systems with standard lime, the optimal temperature is usually between 140 and 150°C. Lower temperatures increase the risk of acid condensates and filter clogging, while higher temperatures can reduce the effectiveness of lime.

Higher relative humidity in the flue gas significantly increases the reactivity of lime towards HCl. For this reason, in dry systems, nebulized water or steam is often injected to condition the flue gas upstream of the reaction.

To ensure compliance with emission limits, systems operate with a reagent excess compared to the theoretical quantity. Typical stoichiometric ratios for dry systems vary between 1.5 and 2.5.

1.4.4 Recirculation of residues

One of the most relevant innovations is the rehydration and recirculation of the residues captured by the baghouse filter. A substantial part of the residues containing unreacted lime is reactivated through humidification or maturation and

reinjected into the flue gas stream. This technique drastically reduces the use of fresh lime, lowers the overall production of solid residues to be disposed of and generates a buffer effect, which allows the system to better manage sudden peaks of acid loads.

1.4.5 Comparison with sodium bicarbonate

Although sodium bicarbonate offers higher reactivity and a stoichiometric ratio close to unit (1.05-1.20), hydrated lime is preferred in many plants because of its lower cost per kilogram and for the lower solubility of its salts (calcium chloride), which are less problematic during storage and disposal compared to sodium salts. In some modern plants, mixed systems are adopted, which can operate with both reagents depending on cost and pollutant load fluctuations (Neuwahl et al., 2010).

1.5 Thesis objectives

In the last few years, research has focused on the development of sorbents characterized by high specific surface area, higher pore volumes and a better distribution of porosity, capable of increasing the lime conversion and reducing reagent consumption. Another line of research concerns the use of limes containing variable quantities of magnesium, whose presence can change both the pore structure and the reaction kinetics of the material.

Despite the many studies conducted, the role of magnesium content in the HCl adsorption capacity is still not completely clear. Some works report improvements in reactivity attributed to the different microstructure of the material, while others underline how the performance depends mainly on the physical properties of the lime rather than on its mere chemical composition.

In this context the present thesis project is positioned, with the objective of comparing the behaviour of two different samples of lime characterized by different formulation and composition, evaluating their capability to retain HCl through laboratory experimental tests and correlating the obtained performances with the physicochemical properties of the materials.

CHAPTER 2: INSTRUMENTATION AND METHODS

2.1 Lime samples used

To conduct the comparison, two different lime samples with different magnesium content and specific surface area were used: C1 and C3.



Figure 1: one of the two lime samples analysed in the tests

2.1.1 Chemical characteristics of the virgin samples

Chemical characterization of the samples was conducted by ICP analysis.

The Inductively Coupled Plasma Optical Emission Spectroscopy (ICP-OES) is an analytical technique for the qualitative and quantitative determination of chemical elements present in a sample.

The working principle of the technique is based on the introduction of the sample, generally dissolved through acid digestion, into an inductively coupled argon plasma, characterized by temperatures between about 6,000 and 10,000 K. Under these conditions, atoms and ions of the elements present in the sample are excited to higher energy levels. During the return to the ground state, each element emits electromagnetic radiation at characteristic wavelengths, which is separated through an optical system and detected by a detector. The intensity of the emitted radiation is directly proportional to the concentration of the element in the sample, allowing quantification through appropriate calibration curves (Charles B. Boss & Kenneth J. Fredeen, 2004; Skoog et al., 2007).

In the case of solid materials, such as the hydrated limes investigated in this study, the results are generally expressed in mg/kg of dry sample, giving the total concentration of the analysed elements, as it is shown in the following summary table of obtained results:

Element	C1 (mg/kg)	C3 (mg/kg)
Ca	563,356	546,407
Mg	2,298	5,387
Na	0	0

The chemical composition of the virgin samples C1 and C3 is mainly represented by the presence of calcium, with concentrations equal to 563 g/kg for C1 and 546 g/kg for C3. This result is compatible with materials mainly composed of calcium hydroxide ($Ca(OH)_2$), typical of hydrated lime.

The main chemical difference between the two materials is given by the magnesium content: the C3 sample is characterized by a higher Mg concentration, equal to 5,387 mg/kg, which is higher than that of C1 (2,298 mg/kg). This difference is coherent with the formulation of the two materials, designed and expressly selected with different magnesium concentrations to evaluate their influence on their behaviour of the materials during the HCl adsorption process.

Sodium was not detected in either sample, indicating the absence of significant contaminations from alkaline salts before the adsorption tests.

2.1.2 Mineralogical composition of the virgin samples

The mineralogical composition of the virgin samples was determined through X-ray diffraction (XRD), a non-destructive analytical technique widely used for the identification and characterisation of the crystal phases present in a material.

The operating principle of XRD is based on the interaction between a monochromatic X-ray beam and the crystal network of the sample. When the incident radiation hits the crystal planes, the X-rays are diffracted following typical angles which depend on the interplanar distance and on the wavelength of the used radiation. The phenomenon is described by the Bragg law:

$$n \cdot \lambda = 2d \cdot \sin\theta$$

where n is the diffraction order, λ is the wavelength, d is the distance between the crystal planes and θ is the diffraction angle. When this condition is satisfied, the diffracted waves constructively interfere generating the characteristic peaks of the diffractogram.

Since each crystal phase has a unique set of diffractions, the comparison of the experimental diffractogram with crystallographic databases allows the identification of their nature. Furthermore, through refinement following the Rietveld method, it is possible to quantitatively determine the weight fraction of the different crystal phases present in the sample (B.D. Cullity & S.R. Stock, 2014; Pecharsky & Zavalij, 2009).

As shown in the graphs below, the XRD analysis of the samples highlighted that both the adsorbents are mainly composed of portlandite (calcium hydroxide, $Ca(OH)_2$), which represents about 90% in weight of the mineralogical composition. In particular, the C1 sample results composed of 89.7 wt.% of portlandite and of 10.3 wt.% of calcite ($CaCO_3$), while the C3 sample contains 90.43 wt.% of portlandite and 9.2 wt.% of calcite. The presence of calcite in both materials is attributable to the partial carbonation of the hydrated lime during the production, handling or storage phases, a commonly observed phenomenon in commercial hydrated limes.

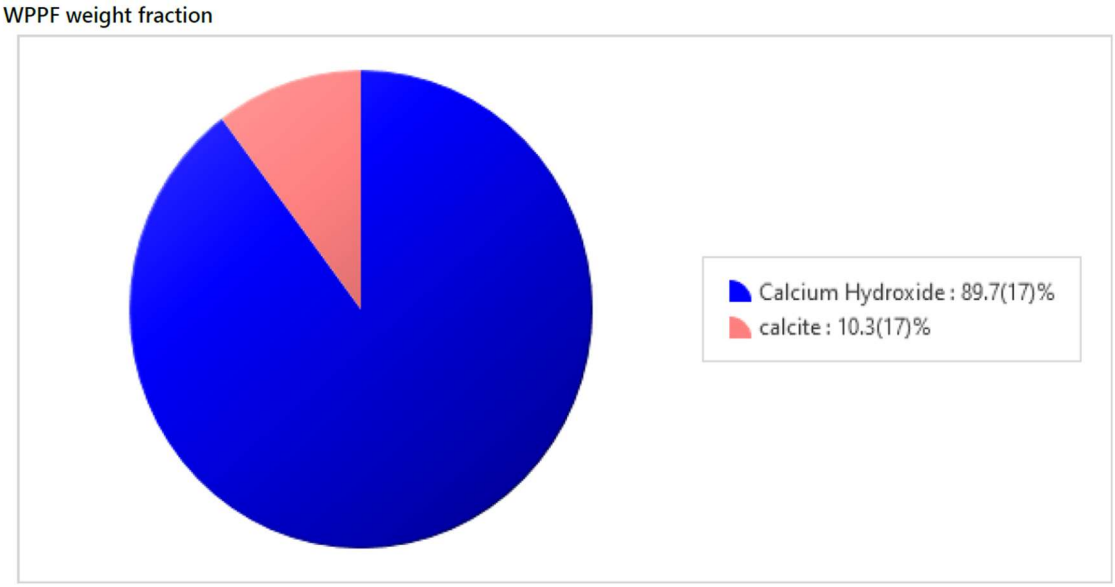


Figure 2: weight fraction mineralogical composition of C1 sample

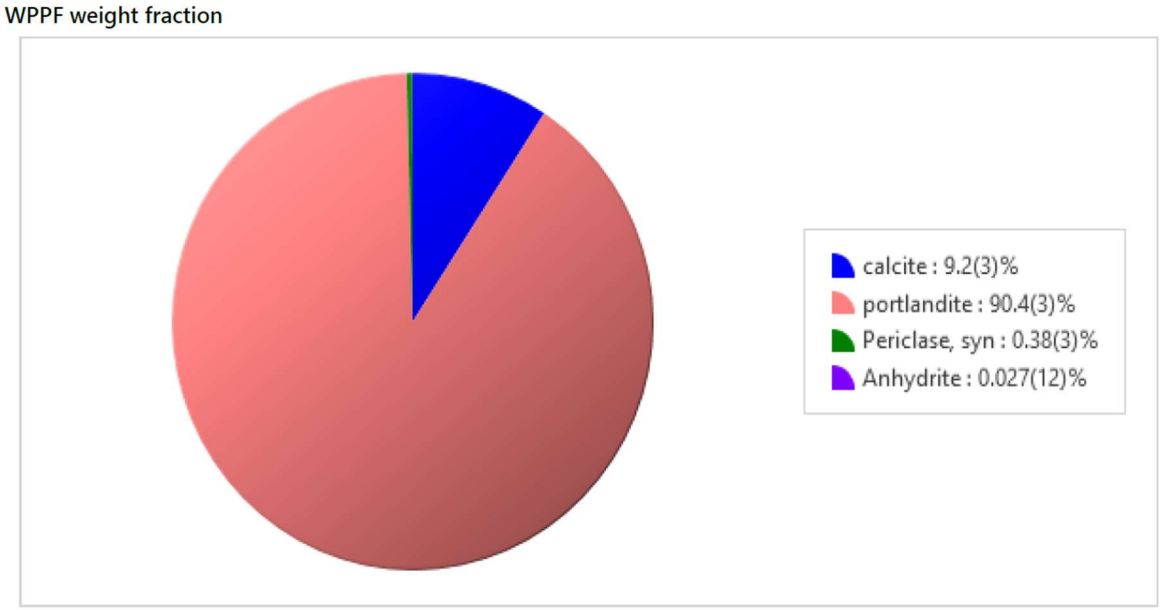


Figure 3: weight fraction mineralogical composition of C3 sample

Differently from the C1 sample, the C3 sample presents traces of periclase (MgO) and anhydrite ($CaSO_4$). The presence of periclase is coherent with the ICP-OES analysis results, which highlighted a magnesium content significantly higher in C3 rather than in C1. The identification of this crystal phase suggests that a part of the magnesium is present as residual magnesium oxide, probably deriving from the raw materials or by the lime production process.

In the C1 sample, instead, there were no traces of crystal phases containing magnesium. This result is not in contrast with the ICP-OES analysis, since this technique determines the total content of the elements present in the sample, independently of their chemical form, while the X-ray diffraction exclusively identifies the crystal phases present in sufficiently high amounts. The detected magnesium in the C1 sample could therefore be distributed inside the portlandite matrix, be present in scarce crystalline phases or in concentrations lower than the detection limit.

Overall, the XRD analysis confirms that the two adsorbents have a very similar mineralogical composition, being both almost exclusively composed of portlandite with a limited amount of calcite. The main difference between the two materials is represented by the presence of periclase in the C3 sample, in agreement with the higher magnesium content highlighted by the ICP-OES. Such compositional difference may influence the behaviour of the two adsorbents during the HCl adsorption process.

2.1.3 Surface area and pore volume of the virgin samples

The physical characterisation of the hydrated lime samples was conducted through nitrogen physisorption of nitrogen using the BET (Brunauer–Emmett–Teller) method, a technique widely used to determine the specific surface area of porous materials.

For each test, a small quantity of powder sample (about 0.2 g) was inserted into the appropriate measurement burettes. Before the analysis, the samples were subjected to a degassing phase at a temperature of 200°C for approximately 1.5 h, with the purpose of removing humidity and any adsorbed molecules from the material's surface which could interfere with the measurements.

At the end of the degassing, the burettes were weighed and later connected to the analysis instrument. During the test, the sample was kept at the temperature of liquid nitrogen (77 K) and subjected to controlled doses of gaseous nitrogen. Nitrogen molecules were progressively adsorbed on the material's surface and inside its porous structure. By measuring the amount of nitrogen introduced and the amount not adsorbed by the sample, it is possible to determine the adsorbed gas

volume at different relative pressures (P/P_0), where P represents the equilibrium pressure and P_0 the nitrogen saturation pressure.

The analysis produces in two experimental isotherms: one for absorption, obtained during the increase of the relative pressure, and one for desorption, recorded during the subsequent decrease of the pressure. The comparison between the two curves provides information about the porous structure of the material.

The specific surface area was determined by applying the Brunauer–Emmett–Teller equation to the linear region of the adsorption isotherm, comprised in the relative pressure interval $0.05 < P/P_0 < 0.30$, in which the BET model is generally valid. From the slope of the line obtained through linearization of the BET equation, the adsorption capacity and, consequently, the specific surface area of the sample, expressed in m^2/g, were calculated (George & Stephen Brunauer, n.d.; Thommes et al., 2015).

In addition to the specific surface area, the instrument software allows the determination of the total pore volume, obtained from the amount of nitrogen adsorbed at high relative pressures, thus providing a complete characterization of the porous structure of the analysed materials.

From the analysis, it emerges that both the samples have a well-developed porous structure, but with different characteristics. The C1 sample shows a specific surface area equal to 41.38 m^2/g, about 41% higher than that of the C3 sample, which has a specific surface area of 29.31 m^2/g. Similarly, the total pore volume is also higher for C1, with a value of 0.244 cm^3/g in adsorption and 0.212 cm^3/g in desorption, while the corresponding values for C3 are 0.201 cm^3/g and 0.178 cm^3/g respectively.

The results therefore show that C1 has a higher specific surface area and pore volume compared to the C3 sample. From a theoretical point of view, a higher specific surface area offers a higher number of available sites for the interaction with gaseous species, while a larger pore volume enhances the diffusion of gas inside the material. These characteristics can influence the behaviour of the two adsorbents

during the HCl adsorption tests and will be considered during the analysis of the experimental results reported in the following chapters.

For both samples, the porous volume calculated from the desorption test is slightly lower than that obtained from the adsorption test. This difference is caused by the hysteresis phenomenon due to the capillary condensation of nitrogen during adsorption and its subsequent evaporation during the desorption process.

2.2 Experimental plant

The experimental tests were conducted using a laboratory plant developed starting from a laboratory prototype previously presented by (Ravina et al., 2023). The apparatus is composed of a feed system for the gaseous mixture, a reactor containing the adsorbent material, a flue gas absorption system at the outlet and an ionic chromatograph used to quantitatively measure the chloride ions present in the obtained solutions.

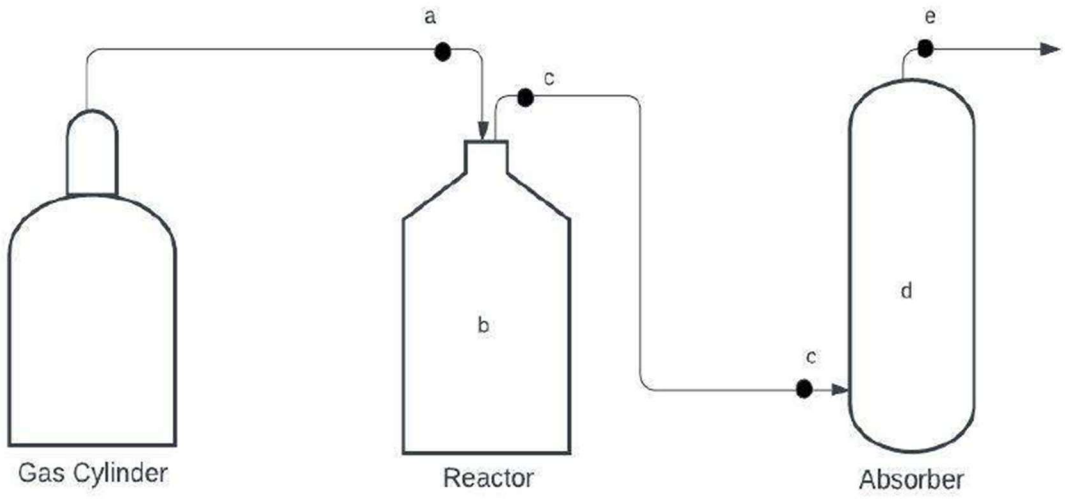


Figure 4: Reference scheme for calculation of chlorides mass balance: (a) total Cl inlet; (b) Cl adsorbed by the solid sorbent; (c) untreated Cl exiting the reactor; (d) Cl adsorbed by the water absorber; (e) residual Cl vented to the atmosphere (Ravina et al., 2023).

The gaseous mixture containing nitrogen and hydrochloric acid is fed to the plant through a pressurized cylinder equipped with a pressure regulator. The feed pressure is kept constant at 0.02 MPa during the tests, while the stream is regulated through a flowmeter set at 0.5 L/min, ensuring reproducible operating conditions between the different experimental tests.



Figure 5: prototype's flowmeter (in the front) and pressure regulator (in the back)

The adsorbent material is placed inside of a small cylindrical support, which is then inserted in the main body of the reactor. The reactor is constantly kept at 150°C by an electrical resistor to simulate the operating conditions inside the flue gas duct of an industrial plant.



Figure 6: small cylindrical support containing the adsorbent material and the filter fabric

For each experiment the adsorbent (C1 or C3) was distributed as homogeneously as possible on a circular support made of PTFE filter fabric (the same type used for baghouse filters), placed inside of the reactor, to promote a uniform gas flow and limiting channeling phenomena.



Figure 7: circular support made of PTFE filter fabric

During the passage of the gaseous mixture, HCl reacts with lime, mainly generating chlorides, while the unretained gas is sent to an absorber containing 100 mL of ultrapure water. Temperature is kept constant to 30°C by a heater throughout the entire volume of the absorber. In this solution, the residual hydrochloric acid is absorbed and dissociated, generating chloride ions, which can later be quantified through ion chromatography.



(a) (b)

Figure 8: absorber used for HCl removal: (a) absorber at the reactor outlet; (b) absorber located inside the heated section at 30°C

The absorber therefore represents the collection system for the HCl not removed by the adsorbent material and would allow the indirect determination of the abatement efficiency of the filter.

The determination of the chloride ion concentration was carried out by ion chromatography (IC), an analytical technique used to separate and quantitatively determine ionic species present in the solution, such as anions and cations. The principle of the technique is based on ions separation through ion-exchange. The sample, dissolved in a liquid phase and, if necessary, filtered and diluted, is injected into a column containing an ion-exchange resin. The ions present interact with the functional groups of the stationary phase with different intensities depending on their charge, dimensions and chemical affinity, determining characteristic retention times for each species.

The eluent transports the analytes through the column to the conductivity detector. The identification of the ions is performed by comparing their retention times with the those of reference standards, while the quantification is carried out using calibration curves obtained by analysing standard solutions of known concentration (Haddad, 2004).

Before conducting the analysis, the chromatograph is stabilized by circulating the eluent until a constant operating pressure is reached. The analyses are conducted using a dedicated method to the determination of chlorides.

The solutions coming from the absorber are directly injected into the instrument through a syringe after an appropriate washing of the injection system with ultrapure water to avoid contamination between consecutive samples.

The chromatograph provides the concentration of chloride ions, expressed in ppm. This value can then be used to calculate the HCl mass present in the solution by multiplying it by the coefficient 1.028 obtained from the equation:

$$\frac{M_{Cl^-}}{M_{HCl}} = \frac{35.45}{36.46} \approx 1.028$$

from which the amount of HCl corresponding to the measured chloride ions can be determined.

The eluent used in the chromatograph is prepared using ultrapure water and the concentrated solution required by the analytical method.

The mass of the adsorbent and of the filters was determined using a high-precision analytical balance.

The drying of the lime was carried out in a furnace, which allows the removal of adsorbed moisture, avoiding its influence on the HCl adsorption capacity and on the reproducibility of the experimental results.

For all the experimental operations, the preparation of the eluent and the dissolution of reacted samples, ultrapure water obtained from a dedicated purification system was used. The use of a very low ionic content water reduces the contribution of analytical blank and improves the accuracy of the chromatographic determinations.

2.3 Experimental procedure

Each test was carried out under functioning extractor hoods, to guarantee adequate extraction of possible gas leakages, although the concentrations used were limited.

Later, the electric resistance was turned on together with the heating system of the absorber. The resistance requires about 30 minutes to stabilize at the operating temperature of 150°C, corresponding to the operating temperature chosen for the experimental tests. At the same time, the ion chromatograph was turned on, which requires about 20 minutes to stabilize under operating conditions before the analyses.

Exception for the blank tests, the lime sample was previously dried in the furnace at 110°C for at least 1.5 h to remove residual moisture and guarantee reproducible initial conditions. The material was then distributed as evenly as possible on a disk made of baghouse filter fabric and subsequently inserted into the reactor. The

homogeneous distribution of the adsorbent allows the generation of a uniform gas flow through the bed of material, limiting channelling phenomena.

After introducing 100 mL of ultrapure water, the absorber was connected to the prototype and placed inside the heated section, where the temperature was maintained at 30°C by the heater.

Once the system preparation was completed, the pressurized cylinder containing the gaseous mixture of nitrogen and hydrochloric acid was opened. During the experimental campaign, two different cylinders were used due to the exhaustion of the first one. The first mixture had a concentration of 469 ppm of HCl, while the second one had a concentration of 483 ppm of HCl. In both cases, the inlet line pressure was regulated at 2 bar.

Subsequently, the pressure regulation valve of the prototype, set at 0.02 MPa, was opened and the flowmeter was regulated at a constant flow rate of 0.5 L/min. The test timing was started when the gas began to bubble inside the absorber, indicating that the gaseous mix was actually passing through the entire system.

At the end of the predetermined experimental time, the gas flow was stopped by closing the flowmeter. A water sample was then collected from the absorber and analysed by ion chromatography to determine the amount of chloride present, from which the mass of HCl not adsorbed (M_d, cf. Figure 4) was calculated. At the same time, both the reacted lime sample and the filter fabric disk used as a support were removed, taking particular care in handling them because of their high temperature, using tongs and protective gloves. The solid samples were subsequently subjected to the further analyses presented in the following chapter.

2.4 Methods for samples analysis

The experimental activity was composed of a series of tests aimed at assessing the HCl adsorption capability of the two filters.

2.4.1 Blank tests

Before the tests with adsorbent material, blank tests were conducted, in which the gas passed through the plant without a filter. The aim of these tests was to determine the absorption efficiency of the absorber and verify the stability of the plant.

The tests were conducted after 15, 30 and 60 minutes of flow of the mixture of hydrochloric acid/nitrogen mixture (HCl concentration equal to 469 ppm).

At the end of each test interval, the solution contained in the absorber was analysed by ion chromatography to determine the chloride ion concentration.

Knowing the plant inlet Cl^- concentration (C_a, known) and the absorbed concentration (C_d, measured by the chromatograph), it was possible to calculate the inlet mass in the plant (M_a) and the absorbed one (M_d) with the following equations:

$$M_a = \frac{P \cdot V}{R \cdot T} \cdot PM_{HCl} = \frac{P \cdot Q \cdot t \cdot C_a}{R \cdot T} \cdot PM_{HCl} = \frac{1\ atm \cdot 0.5\ \frac{L}{min} \cdot t \cdot 469 \cdot 10^{-6}}{0.0821\ \frac{L \cdot atm}{mol \cdot K} \cdot 303\ K} 35.45 \frac{g}{mol}$$

$$M_d = C_d \cdot V = C_d \cdot (0.1 - V_{ci})$$

Where t is the test duration and V_{ci} is the volume extracted from the absorber during the previous tests and used for the ion chromatography measurements. V_{ci} is equal to 0 L for the 15-minute test, 0.002 L for the 30-minute one and 0.004 L for the 60-minute test.

From the values of M_a and M_d, it was possible to calculate the efficiency as follows:

$$\eta = \frac{M_d}{M_a}$$

After conducting the blank tests, the actual tests loaded with the lime samples were carried out to evaluate their performance. They consisted of adsorption tests

(similar to the blank tests, since they involved the measurement of residual C_d in the absorber) and dissolution tests (conducted directly on the lime samples after dissolution in ultrapure water).

2.4.2 Absorption tests on the outlet mass

The absorption tests, similarly to the blank tests, were conducted by passing the gas through the prototype, this time including the lime bed.

To monitor the evolution of the absorption over time, the tests were divided into predefined intervals. At the end of each interval, part of the absorber's solution was withdrawn and analysed through ion chromatography.

Since the chloride concentration progressively increased during the test, the solutions were appropriately diluted before the chromatographic analysis to avoid causing problems to the instrument. Analogously to the blank tests, it was possible to calculate the absorbed mass in the absorber water (M_d) and the injected mass (M_a) to perform a comparison and potentially indirectly evaluate the efficiency of the filter.

2.4.3 Dissolutions on the adsorbed mass

Since the results obtained from the blank and absorption tests were not sufficiently repeatable, it was decided to directly evaluate the amount of chlorine retained by the adsorbent material by developing an experimental procedure based on the dissolution of the reacted sample.

In this case, the material was subjected to HCl adsorption for predefined times of 5, 10, 15, 30, 60, 120 and 180 minutes. At the end of each test, the filter was removed from the plant and replaced with a new sample, making each experiment independent and exclusively referred to its own exposure time.

For each test, about 3 g of reacted sample were withdrawn and later diluted in 300 mL of ultrapure water, maintaining a solid/liquid ratio of 1:100. The suspension was left under stirring for about 21 h, a time deemed sufficient to guarantee the complete dissolution of chlorine salts generated during the reaction between HCl and lime.



Figure 9: stirring samples

The obtained solutions were then analysed through ion chromatography. Before injection into the instrument, appropriate filtrations were done (using 0.020 µm syringe filters) and dilutions (1:2 for samples obtained at 30 and 60 minutes and 1:5 for the ones at 120 and 180 minutes). Moreover, every session, before each analytical session, analyses of a standard solution and an ultrapure water sample were carried out to verify the proper functioning of the instrumentation and guarantee the reliability of the measurements.



Figure 10: 0.20 µm syringe filter

2.4.4 Physicochemical characterization of the reacted samples

Some reacted samples were used for a physicochemical comparison with the virgin ones. In this regard, BET and ICP analysis were conducted using the same methodologies presented in the previous chapters. XRD analysis was performed, but, given the inconsistency of the results, these data were not considered reliable.

CHAPTER 3:
RESULTS AND DISCUSSION

3.1 Blank tests

Five blank tests were conducted, with the last three being consecutively repeated twice to verify the repeatability of the measurements.

For the last three tests, a 1:10 dilution of the samples was introduced before the chromatographic analysis. This change was adopted because in the two previous tests the chloride concentration was high enough to compromise the reliability of the measurements.

The obtained results are reported in the following table as ppm of Cl^- in the aqueous solution at the absorber outlet:

Test number	1	2	3 (average)	4 (average)	5 (average)
C_d at 15 minutes	16.97 ppm	79.32 ppm	21.10 ppm	25.29 ppm	77.55 ppm
C_d at 30 minutes	87.00 ppm	125.42 ppm	78.35 ppm	90.61 ppm	186.18 ppm
C_d at 60 minutes	148.00 ppm	155.97 ppm	256.90 ppm	282.90 ppm	383.00 ppm
Efficiency at 15 minutes	32.3 %	151.2 %	40.2 %	48.2 %	147.8 %
Efficiency at 30 minutes	80.8 %	116.5 %	73.2 %	84.6 %	173.9 %
Efficiency at 60 minutes	67.0 %	70.6 %	117.5 %	129.4 %	175.2 %

As can be seen from the table, the tests showed a very limited repeatability. The chloride concentration measured in the absorber increased with increasing reaction

time in all tests, as expected, but the magnitude of this increase varied considerably between the tests. At 15 minutes, the measured chloride concentrations ranged from about 17 to 79 ppm, while at 60 minutes they ranged from 148 to 383 ppm. This variability is also reflected in the calculated absorber efficiency values, which in many cases were much higher than 100%, a physically impossible result that indicates the presence of measurement errors. This behaviour may be attributed to an underestimation of the HCl inlet concentration, due to a possible stratification of the gas inside of the cylinder, which was close to being exhausted during the tests. Another possible cause is the contamination from chlorides in the analysed samples, the glassware or the analytical system, which may have determined an overestimation of the chloride measured downstream of the absorber. Moreover, a non-uniform distribution of the chloride concentration within the absorber washing water may have contributed to the observed variability between measurements.

Given the high variability of the obtained results, it was not possible to determine the absolute efficiency of the absorber during the blank tests with sufficient confidence. Consequently, the chloride concentrations measured in the washing water cannot be used for quantitative evaluations of the system performance. However, these measurements are still useful for making relative comparisons between the two investigated sorbents (C1 and C3), provided that the subsequent tests show acceptable repeatability.

3.2 Absorption tests on the outlet mass

Initially, four tests were conducted for each adsorbent (C1 and C3) without directly determining the mass adsorbed by the filter. The aim of these tests was twofold: on the one hand, to produce almost completely reacted samples for subsequent dissolution, BET, ICP and XRD analyses; on the other hand, to evaluate the repeatability of the measures concerning the HCl mass at the adsorber outlet in the presence of a filter.

During this first phase of the experimental campaign, however, a progressive deterioration of the reliability of the chromatographic analyses was noticed. In particular, the ion chromatograph showed progressive contamination from chlorides and the chromatographic column, which was close to the end of its useful

life, was no longer guaranteeing sufficiently accurate measurements. Furthermore, the cylinder containing the HCl gaseous mixture, was close to being exhausted; consequently, gas stratification in the first sets of tests cannot be excluded, with a consequent variation in the effective concentration at the system inlet.

For these reasons, the HCl concentration measured at the absorber outlet during the first four sets of tests was not taken into account in the subsequent analyses, since it was not possible to establish with certainty the moment when contamination of the analytical system started to influence the measurements, nor to evaluate the contributions of variations in the inlet HCl concentration. The samples produced during these tests were nevertheless preserved and subsequently used for BET and ICP analyses, since those determinations are not influenced by the unreliability of the chromatographic measurements of the outlet mass.

After the replacement of the chromatographic column and a new calibration of the instrument, two additional sets of tests were conducted for each adsorbent. In these tests samples were collected after 5, 10, 15, 30, 60, 120 and 180 minutes. The collected lime samples were mainly used for the subsequent dissolution tests, which allowed a more direct determination of the HCl mass adsorbed by the material. In parallel, the HCl mass at the absorber outlet was also determined and the results of which are shown in the following tables:

C1

time [min]	5	10	15	30	60	120	180
C_d average [ppm]	0.742	0.598	0.426	3.766	7.146	37.242	54.785
M_a [mg]	1.773	3.545	5.318	10.635	21.270	42.540	63.810
M_d [mg]	0.222	0.179	0.128	1.130	2.144	11.172	16.436

C3

time [min]	5	10	15	30	60	120	180
C_d average [ppm]	0.349	0.396	0.372	4.591	11.045	30.370	65.621
M_a [mg]	1.773	3.545	5.318	10.635	21.270	42.540	63.810
M_d [mg]	0.105	0.119	0.112	1.377	3.313	9.111	19.686

For each experimental session, an ultrapure water sample, to verify the absence of contamination due to the solvent used, a standard solution containing 5 ppm of

chloride ions, to verify the correct functioning of the ion chromatograph, and a 30-minute blank test, to exclude possible contamination coming from the absorber or the experimental line, were conducted.

The measurements obtained after the replacement of the chromatographic column showed lower variability between the two tests compared with the four measurements performed during the first experimental campaign. However, since only two measurements were available, this observation cannot be considered sufficient to assess their repeatability. The chloride concentration measured in the absorber could provide useful information on the fraction of HCl that was not retained by the C1 or C3 sample, but only if the measurements are sufficiently repeatable and the absorber efficiency is reliably determined for each reaction time. Since these data alone are not sufficient to determine those parameters, more tests were conducted directly on the lime samples.

3.3 Dissolution tests on the adsorbed mass

Dissolution tests allowed the direct determination of the HCl mass adsorbed by the lime samples during the absorption tests. For each adsorbent (C1 and C3) two independent tests were carried out and, for each test, two chromatographic analyses were consecutively done to verify the repeatability of the measurements.

Analogously to the previous tests, before the analyses, both the used ultrapure water and a standard solution containing a known chloride concentration were analysed, to exclude possible contamination of the solvent or of the analytical system.

The 3 g samples were kept under stirring for about 21 h, using a 1:100 dilution, and subsequently filtered through syringe filters with porosity equal to 0.20 μm. The solutions obtained in this way were analysed by ion chromatography.

The results reported in the following tables represent the average of the Cl^- concentration measured in the two sets of tests:

C1

time [min]	5	10	15	30	60	120	180
C_b average [ppm]	4.228	8.064	10.934	16.225	33.114	57.565	86.698
M_a [mg]	1.773	3.545	5.318	10.635	21.270	42.540	63.810
M_b [mg]	1.268	2.419	3.280	4.868	9.934	17.270	26.009
Absorption %	71.564	68.240	61.684	45.769	46.705	40.596	40.761

C3

time [min]	5	10	15	30	60	120	180
C_b average [ppm]	9.968	12.503	16.046	19.390	38.018	61.693	103.164
M_a [mg]	1.773	3.545	5.318	10.635	21.270	42.540	63.810
M_b [mg]	2.990	3.7508	4.814	5.817	11.405	18.508	30.949
Absorption %	100.000	100.000	90.529	54.697	53.621	43.507	48.502

The results show that the adsorbed mass progressively increases with the exposure time, as expected, while the adsorption percentage (M_b/M_a ratio) follows a different trend. In the first minutes of the test the adsorption is quite high, with values over 60–70% for both the materials and close to 100% in the case of C3 sample. As the reaction time increases, however, this percentage progressively decreases until it stabilises around 40–50% after about 60–120 minutes. This trend suggests that the adsorption process is very quick at the beginning and then progressively decreases with the progress of the reaction.

The progressive reduction of the adsorption percentage can be explained considering the reaction mechanism between HCl and $Ca(OH)_2$. In the initial phases of the test the surface of the particles is completely available and presents a high number of reactive sites easily accessible. In these conditions, HCl quickly reacts with calcium hydroxide, determining a high adsorption rate and, consequently, very high removal percentages.

As the reaction progresses, the amount of available $Ca(OH)_2$ on the most exposed to the gas flow surfaces progressively decreases and a layer of reaction products mainly composed of $CaCl_2$ is generated. This layer represents an additional resistance to the mass transfer, since the HCl molecules must diffuse through it before reaching the still-unreacted core of the material. Consequently, the reaction velocity progressively decreases and an ever-increasing fraction of HCl passes

through the filter without reacting, defining the reduction of the adsorption percentage experimentally observed.

This behaviour is coherent with the shrinking core model, commonly used to describe the reaction between lime-based sorbents and acid gases. According to this model, the reaction is initially controlled by surface kinetics, while increasing the degree of conversion, the diffusion of the reagents through the reaction products layer plays an increasingly important role. The progressive reduction of the adsorption percentage observed for both the samples results then compatible with the transition from a surface reaction-controlled regime to a diffusion-controlled regime. Such an interpretation is coherent with what reported by (Antonioni et al., 2016).

These interpretations are furthermore supported by the BET analyses presented in the next paragraph, which show an evident reduction of the specific surface area and of the pore volume after the reaction. Such results confirm that the generation of reaction products involves a progressive occlusion of the porous structure of the sorbent, increasing the diffusional limitations and reducing the adsorption rate at longer exposure times.

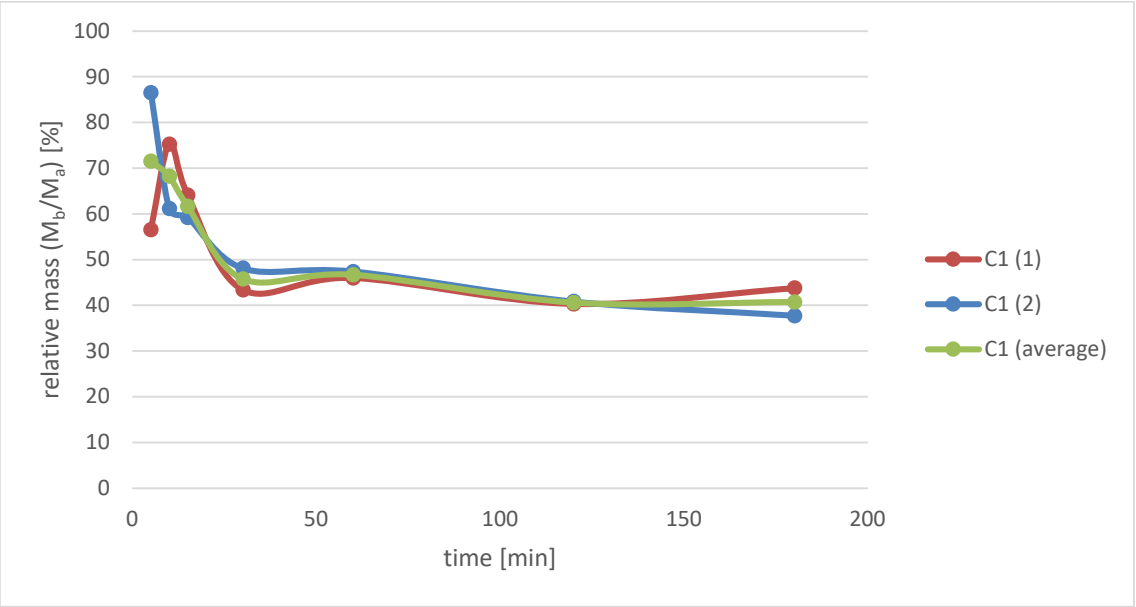
It is appropriate to observe that, in these experimental tests, the sorbent was employed in large excess compared to the stoichiometric amount of HCl feed. For the maximum experimental duration of 180 min, the theoretical amount of $Ca(OH)_2$ required to react with the HCl fed to the system was estimated to be approximately 0.3109 g, compared with the 3.0 g of sorbent actually used. Therefore, the amount of sorbent introduced was approximately 9.65 times higher than the theoretical amount consumed during the test, corresponding to the theoretical consumption of only about 10.4% of the initial $Ca(OH)_2$. Assuming a constant reaction rate, the complete theoretical consumption of the 3.0 g of $Ca(OH)_2$ would have required approximately 29 h. Therefore, it is reasonable to consider that a significant amount of $Ca(OH)_2$ was unreacted also at the end of the tests. The reduction of the adsorption percentage cannot therefore be exclusively attributed to the progressive consumption of the available $Ca(OH)_2$. An additional factor which could have contributed to such a behaviour is a non-perfect distribution of the gaseous stream inside the lime bed. In these conditions it is possible that the gas preferentially

passed through some regions of the bed (channelling), determining a higher conversion of the most exposed particles, while others remained only partially exploited. Although the present work cannot experimentally verify such a hypothesis, non-uniform flow distribution phenomena are frequently reported in the literature for fixed-bed reactors and may have contributed, together with the diffusional limitations inside the single particles, to the progressively observed reduction of the adsorption percentage (Augier et al., 2010; Gunjal et al., 2005).

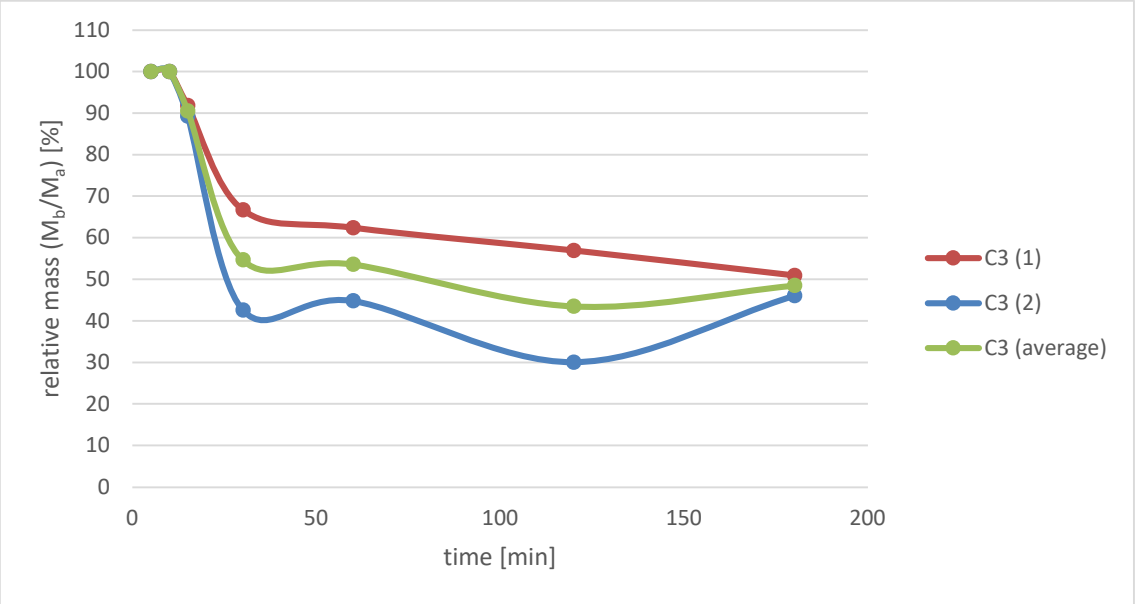
In the case of the C3 sample, the samplings performed after 5 and 10 minutes gave adsorbed mass values (M_b) slightly over the HCl inlet mass in the system (M_a), obtaining adsorption percentages higher than 100%, which have no physical meaning. Such discrepancies are attributable to the limited amount of HCl involved in short-duration tests, for which even modest experimental errors can produce significant percentage variations. Possible causes include the presence of residual traces of chlorides in the water used for the dilutions, small inaccuracies in the preparation of the dilutions, as well as slight fluctuations in the gas flow rate during the tests. For this reason, in the data processing, the percentage of adsorption in both cases was assumed to be 100%.

A comparison between the two adsorbents underlines how the C3 sample systematically presents higher adsorbed chloride masses compared to the C1 sample (Graphs 1 and 2). Consequently, the adsorption percentage generally results higher, with differences between 4 and 9% for the majority of test times, while in the first phases of the experiment the gap results even more evident. This behaviour suggests a higher initial adsorption capacity of the C3 sample, as it will be discussed in the following sections dedicated to the reacted materials characterisation.

The trend of the adsorption percentage (M_b /M_a) is shown in the following graphs:



Graph 1: relative Cl^- mass adsorbed by C1



Graph 2: relative Cl^- mass adsorbed by C3

In both cases it is possible to notice a rapid decrease of the adsorption percentage between 15 and 30 minutes, followed by a progressive stabilisation towards an almost constant value. The local oscillations observable in some points in the graphs, as for example in the C1 tests at 5 and 30 minutes and in the C3 tests at 30 and 120 minutes, are attributable to common experimental variability and to the same sources of error previously discussed.

The results of the dissolution tests also allow the estimation of the HCl mass reaching the absorber (M_c), calculated by difference between the injected mass into the system (M_a) and the mass adsorbed by the lime (M_b). Combining this information with the absorber's outlet mass (M_d) it would then be possible to calculate the absorber's efficiency in the different time intervals. This procedure however requires to assume that the entire amount of generated $CaCl_2$ is completely dissolved during the dissolution process. This hypothesis represents an approximation, since a small fraction of the products can be trapped inside of the lime's porous structure, without being completely extracted.

The calculated efficiencies are shown in the following tables:

C1

time [min]	5	10	15	30	60	120	180
absorber efficiency test 1	12.31%	9.47%	2.81%	8.95%	6.58%	19.32%	9.00%
absorber efficiency test 2	22.46%	2.66%	1.45%	3.89%	6.02%	10.11%	19.45%

C3

time [min]	5	10	15	30	60	120	180
absorber efficiency test 1	n.a.	n.a.	10.25%	15.92%	17.35%	12.44%	24.53%
absorber efficiency test 2	n.a.	n.a.	5.20%	5.83%	7.00%	12.76%	15.82%

The observed differences between the two replicated tests still show a significant variability, which does not allow the determination of the absolute value of the absorber's efficiency for each temporal interval with sufficient reliability. These results therefore confirm the observation made for the blank tests, showing that the absorber measurements are mainly suitable for a qualitative and comparative analysis rather than an accurate quantitative determination of the absolute efficiency.

3.4 BET analysis

The BET analysis was done also on the hydrated lime samples of about 0.5 g withdrawn at the end of an HCl adsorption test, after a reaction time of 330 minutes, to evaluate the changes in the porous structure induced by the reaction.

The obtained results are shown in the following table:

Sample	BET surface (m^2/g)	Adsorption pore volume (cm^3/g)	Desorption pore volume (cm^3/g)
C1 reacted	8.88	0.0624	0.0520
C3 reacted	7.69	0.0384	0.0335

Both the samples show an evident specific surface area and total pore volume reduction compared to the corresponding virgin materials. Such a behaviour is attributable to the reaction between HCl and hydrated lime, which mainly leads to the formation of calcium chloride in solid phase, which tends to settle on the particles' surface and inside the pore network. This phenomenon determines a progressive occlusion of the pores and a consequent reduction of the accessible surface for the nitrogen adsorption.

To highlight the extent of the variations, the following tables show the comparison between virgin materials and the reacted ones:

Sample	Virgin surface (m^2/g)	Reacted surface (m^2/g)	Variation
C1	41.38	8.88	−78.5%
C3	29.31	7.69	−73.7%

Sample	Virgin pore volume (cm^3/g)	Reacted pore volume (cm^3/g)	Variation
C1	0.2439	0.0624	−74.4%
C3	0.2014	0.0384	−80.9%

It can be observed that the C1 sample, even if starting from a significantly higher specific surface area compared to C3 (41.4 vs. 29.3 m^2/g), after the reaction it retains a slightly higher surface (8.88 m^2/g vs. 7.69 m^2/g). Similarly, the residual pore volume is also higher in the C1 sample (0.062 cm^3/g vs. 0.038 cm^3/g).

The percentage reductions result however comparable for both the materials, indicating that the HCl reaction substantially modifies the porous structure independently from the considered sample. In particular, the specific surface area decreases by about 75–80%, while the total pore volume decreases of over 74% for C1 and of about 81% for C3. This suggests that the generation of the reaction products involves a significant part of the accessible surface and of the initially available pore network.

The difference between the pore volumes obtained from the adsorption and desorption branches is noticeable also in the reacted samples, indicating that, despite the substantial reduction of the porosity, the material still keeps a residual porous structure. However, the amount of pores accessible to nitrogen results much lower compared to the virgin samples.

Overall, the results confirm that the prolonged exposure to HCl causes deep modifications in the physical characteristics of the hydrated lime. The marked reduction of the specific surface area and of the pore volume provides experimental evidence of the occurrence of the reaction and of the progressive occupation of the pores by the generated products, a phenomenon which can limit the gaseous reagent diffusion towards the still reactive core of the particles and contribute to the progressive capture efficiency reduction observed in the adsorption tests.

3.5 ICP analysis

The ICP-OES analysis was conducted on about 0.5 g of the C1 and C3 samples after 330 minutes of exposure to the gaseous mixture containing HCl, to evaluate the variations in the elemental composition after the adsorption process.

Calcium is still the main element in both the samples after the reaction, even if a reduction of its concentration can be observed compared to the virgin materials. In particular, the Ca content goes from 563,356 mg/kg to 369,059 mg/kg in the C1 sample and from 546,407 mg/kg to 423,532 mg/kg in the C3 sample, corresponding to reductions of about 34% and 22%, respectively.

A similar reduction is observed for magnesium as well. In the C1 sample the Mg concertation lowers from 2,298 mg/kg to 938 mg/kg, while in the C3 sample it decreases from 5,387 mg/kg to 3,497 mg/kg, with decreases equal to about 59% and 35%, respectively. Despite this reduction, the C3 sample maintains a significantly higher magnesium content compared to C1, according to the different initial formulation of the two adsorbents.

The reduction of the calcium and magnesium concentrations is compatible with the hydrochloric acid neutralization reactions by the alkaline-earth hydroxides present in the hydrated lime. During the adsorption process, in fact, HCl reacts with $Ca(OH)_2$ and with the species containing magnesium, generating the corresponding chlorides ($CaCl_2$ and $MgCl_2$), characterised by a high solubility in water. Consequently, a part of these reaction products can be removed during the preparation of the samples for the ICP-OES analysis, resulting in a decrease in the elemental content of the solid residue. Furthermore, the generation of new compounds and the increase of the sample mass following the adsorption of HCl contributes to modify the concentration of the elements expressed in mg/kg.

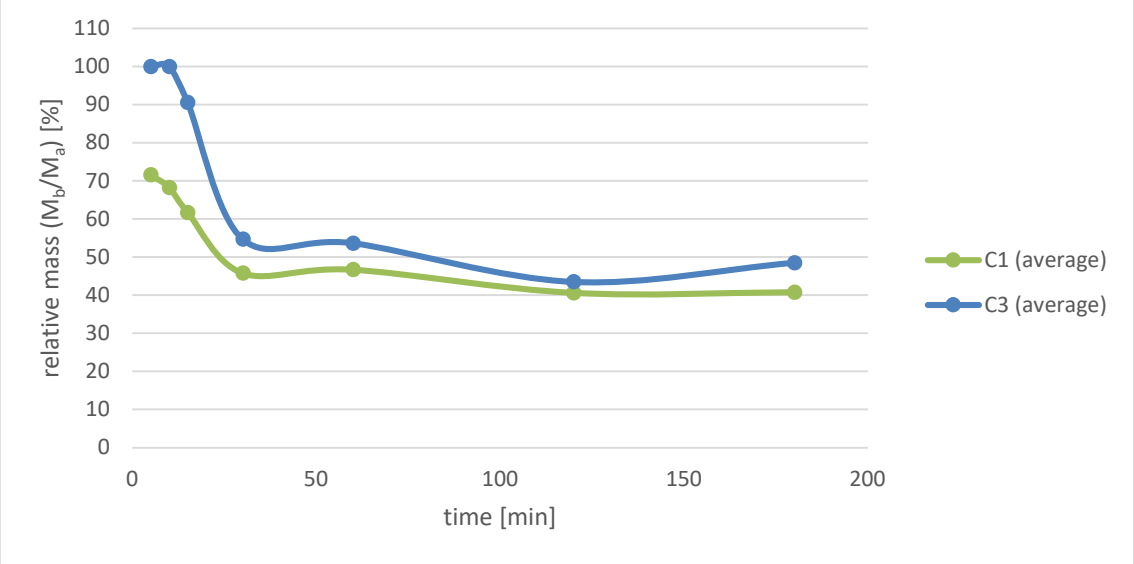
Another noticeable aspect concerns the appearance of sodium in the reacted samples. While in the virgin materials Na was not detectable, after the treatment concentrations equal to 2,774 mg/kg for C1 and to 2,114 mg/kg for C3 are measured. Since sodium is not present in the gaseous mixture used during the tests, its presence is likely attributable to induced contaminations during the preparation or the manipulation of the samples, or to traces present into the reagents or in the water used in the experimental phase.

The comparison between the two materials highlights that the C3 sample keeps, after the treatment, higher concentrations of calcium and magnesium compared to C1. In detail, the residual calcium content is equal to about 424 g/kg in C3, against 369 g/kg in C1, while the magnesium content stays almost four times higher (3,497 mg/kg vs. 938 mg/kg). Also considering the obtained results on the virgin samples, it emerges that the C3 sample undergoes a lower percentage reduction for both calcium and magnesium compared to C1. Such a behaviour suggests a higher conservation of the species containing Ca and Mg in the C3 material at the end of the adsorption test. However, the ICP analysis exclusively gives information about the

overall elemental composition of the sample and does not allow the identification of the present chemical phases, nor to distinguish the elements still present as hydroxides from the ones converted to the respective chlorides.

3.6 Comparison between C1 and C3 samples

The comparison of the obtained results highlights how the two adsorbents present a qualitatively similar behaviour during the HCl adsorption process, but with significant quantitative differences. In both cases the adsorbed mass progressively increases with the exposure time, while the ratio between the adsorbed and the injected mass (M_b /M_a) rapidly decreases during the first phases of the test and then tends to an almost constant value. This trend reflects the progressive slowdown of the reaction kinetics, attributable to the formation of reaction products and to the consequent diffusional limitations previously discussed.



Graph 3: comparison of the relative Cl^- mass adsorbed by the two samples

From the direct comparison of the two curves, it emerges that the C3 sample maintains, for the whole duration of the test, higher values of the M_b/M_a ratio compared to the C1 sample. The difference is particularly highlighted in the initial phases of the experiment, during which C3 reaches an almost complete HCl adsorption, while at longer times the advantage is reduced, remaining in the order of a few percentage points. Overall, the results show a higher HCl capture capacity by the C3 samples.

The interpretation of this behaviour results particularly interesting if compared with the characterisation analyses. The BET tests conducted on virgin materials have in fact highlighted that the C1 sample has a higher specific surface area and pore volume compared to the C3 sample. If the process was exclusively driven by the availability of accessible surface, better performance would be expected for C1. The experimental results show instead the opposite behaviour, suggesting that the initial specific surface area is not the only parameter responsible for the efficiency of the adsorption.

ICP analyses show also that the C3 sample presents an initial magnesium content significantly higher than C1 and, even after the reaction, it maintains higher concentrations for both calcium and magnesium. Although ICP does not allow the directly identification of the chemical species present, those results confirm that the two adsorbents have a different initial composition, attributable to the different formulation of the material. It is then likely that this composition influences not only the superficial reactivity, but also the evolution of the porous structure during the reaction, contributing to the better performances observed for the C3 sample.

The BET analyses conducted on the reacted samples show in fact that both the materials undergo a marked reduction of the specific surface area and of the pore volume, confirming the progressive occlusion of the porous structure due to the formation of reaction products. Although this evolution is common to both adsorbents, C3 keeps a higher adsorption capability during the entire test, indicating that the different observed behaviour cannot be exclusively attributed to the variations of the specific surface area.

Overall, the obtained results show that the C3 sample represents the most effective adsorbent among those investigated for the removal of HCl in the adopted operational conditions. Its best performance appears to be mainly attributable to the different composition of the material rather than to a higher initial specific surface area. These results highlight how, in the sorbent design for the acid gases abatement, chemical properties and reactivity of the material can assume a role at least as important as the mere physical characteristics of the porous structure.

CHAPTER 4: CONCLUSIONS

The present thesis work had the objective of evaluating the hydrochloric acid adsorption capacity of two samples of hydrated lime, named C1 and C3, characterised by different magnesium contents and physical properties. The study was conducted through a laboratory experimental campaign finalised to both the determination of the trend of the adsorption along the time and the physicochemical characterisation of the materials before and after the reaction with HCl.

The preliminary tests conducted through the monitoring of the HCl mass at the absorber outlet highlighted a limited repeatability of the results. The presence of contaminations in the chromatograph, the progressive deterioration of the analysis column and the possible variation of the feed gaseous mixture, did not allow the determination of the absolute efficiency of the absorber with sufficient reliability. Despite these limitations, the experimental activity allowed the identification and the correction of the main sources of errors, progressively improving the reliability of the experimental procedure.

To overcome these limitations, a new methodology based on the dissolution of the reacted samples and the subsequent determination of chlorides through ion chromatography was developed. This approach allowed a more direct evaluation of the HCl mass actually retained by the sorbent, representing the main comparison tool between the materials.

The obtained results show that both samples are characterised by a rapid adsorption at the beginning of the tests, followed by a progressive decrease of the

retained HCl percentage until almost stable values are reached. This behaviour is consistent with the shrinking core model, according to which the reaction is initially controlled by surface kinetics, while subsequently, diffusion limitations due to the formation of reaction products and the occlusion of the porous structure take on a predominant role.

The comparison between the two adsorbents highlights how the C3 sample showed, in the majority of the tests, a higher adsorption capability than C1. This behaviour appears particularly evident in the initial phases of the experiments, while it tends to decrease with the increasing exposure time. Considering that C3 has a lower initial specific surface area compared to C1, but a higher magnesium content, the results suggest that the latter may positively contribute to the material's behaviour against HCl. However, based on the obtained results, it is not possible to exclusively attribute this difference to the magnesium presence, since the lime reactivity depends on the interaction of many factors, including the porosity distribution, the material's microstructure and the operating conditions of the test.

The BET analyses conducted on the reacted samples highlighted a drastic decrease of the specific surface area and of the total pore volume compared to the virgin materials. These results experimentally confirm that the reaction with HCl entails a progressive occlusion of the porous structure, reducing the amount of accessible sites and limiting the diffusion of the reagent towards the still unreacted core of the particles. The ICP analyses also showed a decrease of the calcium and magnesium concentration and the appearance of sodium in the reacted samples, confirming the chemical modifications following the adsorption process and the formation of reaction products.

Overall, the carried-out work, has allowed a deeper understanding of the behaviour of two different types of hydrated lime towards the adsorption of hydrochloric acid and to correlate the observed performance with the physicochemical characteristics of the materials. Although some experimental limitations emerged, the developed methodology allowed the acquisition of results consistent with the mechanisms described in the literature and to highlight performance differences between the two adsorbents.

As a possible future development, it would be appropriate to repeat the tests using a further optimised experimental line, with a feed system of the gaseous mixture capable of ensuring a constant HCl concentration and a more uniform distribution of the flow through the lime bed. Another improvement may consist of the implementation of a system for the direct and continuous measurement of the HCl concentration at the prototype inlet to determine with higher accuracy the amount of reagent actually fed during each test and to reduce the uncertainty associated with the calculation of the abatement efficiencies. It would also be appropriate to increase the number of experimental tests and their replications, in particular for the dissolution tests and the physicochemical analyses, in order to improve the statistical robustness of the results and more reliably evaluate the performance differences between the different adsorbents. Finally, the extension of the study to a higher number of samples characterised by different magnesium contents, together with the use of other characterisation techniques, such as the X-ray diffraction (XRD) applied also to the reacted samples and the scanning electron microscopy (SEM), would allow further investigation of the reaction mechanisms and to clarify more precisely the role of magnesium in the performance of hydrated lime for the abatement of HCl.

REFERENCES BIBLIOGRAPHY

Antonioni, G., Dal Pozzo, A., Guglielmi, D., Tugnoli, A., & Cozzani, V. (2016). Enhanced modelling of heterogeneous gas–solid reactions in acid gas removal dry processes. *Chemical Engineering Science*, *148*, 140–154. https://doi.org/10.1016/J.CES.2016.03.009

Augier, F., Idoux, F., & Delenne, J. Y. (2010). Numerical simulations of transfer and transport properties inside packed beds of spherical particles. *Chemical Engineering Science*, *65*(3), 1055–1064. https://doi.org/10.1016/J.CES.2009.09.059

B.D. Cullity, & S.R. Stock. (2014). *Elements of X-Ray Diffraction*. Pearson Education Limited.

Charles B. Boss, & Kenneth J. Fredeen. (2004). *Concepts, Instrumentation and Techniques in Inductively Coupled Plasma Optical Emission Spectrometry* (PerkinElmer, Ed.; 3rd ed.). www.perkinelmer.com

George, A., & Stephen Brunauer, B. (n.d.). *03s ADSORPTION OF GASES IN MULTIMOLECULAR LAYERS 300 [CONTRIBUTION FROM THE BUREAU OF CHEMISTRY AND Sons Adsorption of Gases in Multimolecular Layers*.

Gunjal, P. R., Ranade, V. V., & Chaudhari, R. V. (2005). Computational Study of a Single-Phase Flow in Packed Beds of Spheres. *AIChE Journal*, *51*(2), 365–378.

Haddad, P. R. (2004). Ion chromatography. *Analytical and Bioanalytical Chemistry*, *379*(3), 341–343. https://doi.org/10.1007/s00216-004-2572-7

M. Giugliano; S. Cernuschi. (2014). *Trattamento delle emissioni in atmosfera*.

Neuwahl, F., Cusano, G., Benavides, J. G., Holbrook, S., & Roudier, S. (2010). *Best Available Techniques (BAT) Reference Document for Waste Incineration*.

Pecharsky, V. K., & Zavalij, P. Y. (2009). *Fundamentals of Powder Diffraction and Structural Characterization of Materials* (Springer, Ed.; 2nd ed.).

Ravina, M., Marotta, E., Cerutti, A., Zanetti, G., Ruffino, B., Panepinto, D., & Zanetti, M. (2023). Evaluation of Ca-Based Sorbents for Gaseous HCl Emissions Adsorption. *Sustainability (Switzerland)*, *15*(14). https://doi.org/10.3390/su151410882

Skoog, D. A. ., Holler, F. James., & Crouch, S. R. . (2007). *Principles of instrumental analysis*. Thomson Brooks/Cole.

Thommes, M., Kaneko, K., Neimark, A. V., Olivier, J. P., Rodriguez-Reinoso, F., Rouquerol, J., & Sing, K. S. W. (2015). Physisorption of gases, with special reference to the evaluation of surface area and pore size distribution (IUPAC Technical Report). *Pure and Applied Chemistry*, *87*(9–10), 1051–1069. https://doi.org/10.1515/pac-2014-1117